ADVANCES IN SPATIAL SNOW MODELING IN MOUNTAIN TERRAIN

Stefan W. Kienzle[1]

ABSTRACT

Snow modeling is a demanding task in itself, but is even more demanding in complex terrain such as the Rocky Mountains. Snow modeling is carried out here with the ACRU agro-hydrological modeling system. A critical advancement was the development of a new method to separate snow and rain (Kienzle, 2008). As a further improvement, a new GIS based method that determines two daily minimum and maximum temperatures, based on incoming radiation calculations and leaf area index adjustments, is presented. This results in a daily, lapse rate dependent, air temperature to determine the precipitation type (snow or rain), and a near-ground air temperature to determine snow melt and evapotranspiration rates. A drawback in most distributed hydrological models is that area calculations are based on the horizontal plane rather than the sloped area. A method is presented to use two area calculations for each hydrological response unit: a horizontal area, which is used for precipitation input calculations, and a larger sloped area, which is used for all other hydrological processes, including interception, sublimation, snow melt, soil moisture, or groundwater recharge.

INTRODUCTION

The ACRU Agro-Hydrological Modeling System

The ACRU agro-hydrological modeling system (from here on referred to simply as ACRU) has been developed in the Agricultural Catchments Research Unit (ACRU), Department of Agricultural Engineering (now the School of Bioresources Engineering and Environmental Hydrology) at the University of KwaZulu-Natal, Republic of South Africa, since the late 1970s (ACRU, 2007). The developers (Schulze, 1995; Smithers and Schulze, 1995) refer to the ACRU model as a multi-purpose, multi-level, integrated physical-conceptual model that can simulate total evaporation, soil water and reservoir storages, land cover and abstraction impacts on water resources and streamflow at a daily time step. The ACRU model revolves around multi-layer soil water budgeting with specific variables governing the atmosphere-plant-soil water interfaces. Runoff is generated as quick flow, which responds to the magnitude of daily rainfall in relation to dynamic soil water budgeting, i.e. the antecedent moisture conditions.

In 2006, a snow model was incorporated to extend ACRU's limitation for applications in snow-free regions to virtually anywhere in the world. The snow model incorporates a novel approach to separate precipitation into snow and rain, which was developed based on almost a 1000 years of daily climatic records from southern Alberta (Kienzle, 2008). Subsequent snow processes, such as canopy interception, sublimation, metamorphosis, or change in albedo and density, are simulated in a physically explicit manner. The snow melt simulation is currently based on a degree-day factor, which is determined on a daily basis from incoming radiation and albedo estimates.

ACRU is not a parameter fitting or optimizing model, as all variables are estimated from the physical characteristics of the watershed. When not all required variables are available, they are estimated within physically meaningful ranges based either on the literature or local expert knowledge. Spatial variation of rainfall, soils and land cover is facilitated by operating the model in distributed mode, in which case the catchment is subdivided into either small subwatersheds or hydrological response units (HRUs), each representing a relatively homogenous area of hydrological response.

ACRU has been used extensively in South Africa for water resource assessments (Everson, 2001; Kienzle *et al*, 1997; Schulze *et al.*, 2004), flood estimation (Smithers *et al.*, 1997; 2001), land use impacts (Kienzle and Schulze, 1991; Tarboton and Schulze, 1993), nutrient loading (Mtetwa *et al*., 2003), climate change impacts (New, 2003; Schulze *et al.*, 2004), or irrigation supply (Dent, 1988) and irrigation impact (Kienzle and Schmidt, 2008), and often requires extensive GIS pre-processing (Kienzle, 1993; 1996; Schulze *et al.*, 1990). Model manuals are available through the internet at the ACRU web page (ACRU, 2007; Schulze, 1989; 1995; Smithers and Schulze,

Paper presented Western Snow Conference 2009
[1] Department of Geography, University of Lethbridge, Lethbridge, Alberta, Canada - (stefan.kienzle@uleth.ca)

1995). ACRU is currently applied to estimate snow fall changes in southern Alberta under climate change conditions, and to estimate a wide range of water resources impacts on the upper St. Mary watershed in Montana (approx. 1000 km^2) and the upper North Saskatchewan watershed (approx. 20,000 km^2). Some examples presented here are from the upper St. Mary watershed, Montana.

Preparing ACRU variables for watersheds with a large proportions of high mountain ranges typically result in a number of challenges, such as a large number of HRUs (often exceeding a 1000), radiation calculations, and spatially explicit adjustments for daily minimum and maximum temperatures, sunshine hours, and wind speed.

Snow Modeling

For successful snow simulations on a watershed scale, a number of important computations are required, including spatial modeling of minimum and maximum temperatures, separation of precipitation into snow and rain, snowpack development and metamorphoses, and snow melt. The calculation of the required daily input variables, such as incoming radiation, minimum and maximum temperatures, albedo, and also the delineation of hydrological response units, are based on sometimes complex spatial analyses using a GIS.

OBJECTIVES

Preparing ACRU variables for watersheds with a large proportions of high mountain ranges typically result in a number of challenges, in particular the extrapolation of climate variables from a single climate station to a physiographically diverse watershed, which is typically subdivided into hundreds of hydrological response units (HRUs). A further common problem is the under-estimation of HRU areas in mountainous terrain, as area calculations are based on the horizontal plane rather than the true, sloped area. Three novel approaches on improved spatial representation of climate variables are presented here, which are all interlinked:

1. separation of precipitation into rain and snow (Kienzle, 2008),
2. incorporation of two daily temperatures to distinguish between temperatures that govern precipitation type and temperatures that govern hydrological processes on the ground, such as evapotranspiration and snowmelt, and
3. incorporation of two areas for each HRU, a horizontal area, required to determine precipitation depth, and the true sloped area, required for the estimation of all hydrological outputs.

SEPARATION OF DAILY PRECIPITATION INTO SNOW AND RAIN

There are currently four different approaches available to separate precipitation into snow and rain based on air temperature.

- One type of approach uses the static threshold temperature method. Based on this method, 100% of snowfall is assumed when temperatures are below the threshold temperature, otherwise 100% rainfall is assumed.
- Another approach uses a gradual change of the proportion of snow and rain based on a linear transition over several degrees, such as the Canadian UBC Watershed Model (Pipes and Quick, 1977). Others, such as the U.S. Army Corps of Engineers (1956) or Braun (1989), use slightly different linear equations.
- A third approach, applied in USGS's PRMS model (Leavesley *et al.*, 1983), is more complex. Here, the snow proportion is a function of daily minimum and maximum temperatures. In addition, a second threshold temperature can be defined where all precipitation is regarded as rain, irrespective of the daily maximum temperature.
- A fourth method uses an S-shaped curve instead of a linear transition. The shape of the curve is determined by the threshold temperature and the range of temperatures within which mixed precipitation may occur (Kienzle, 2008). Using three objective functions to compare the four methods with observed daily records, totalling over 963 years, it was revealed that this method resulted in significantly higher coefficients of determinations. Most importantly, Kienzle (2008) confirmed that a strong seasonal oscillation exists of the threshold temperature, which can be estimated using a sine equation.

Similar to observations made in the European Alps (L'hote *et al*., 2005), Switzerland (Rohrer, 1989), the South American Andes (L'hote *et al*., 2005), the USA (Auer, 1974; Fassnacht *et al*., 2001), Finnland (Vehviläinen, 1992) and Norway (Forland, 2003), the investigation in south-western Alberta, Canada, of the separation of precipitation into snow and rain as a function of air temperature resulted in an s-shaped curve. The shape of the curve is quite consistent for the 15 climate stations investigated (Figure 1). The shape of the curve was

mathematically described, using two observable variables: the threshold temperature T_T, where 50% of the precipitation falls as snow, and the temperature range T_R, within which the transition from snow to rain occurs.

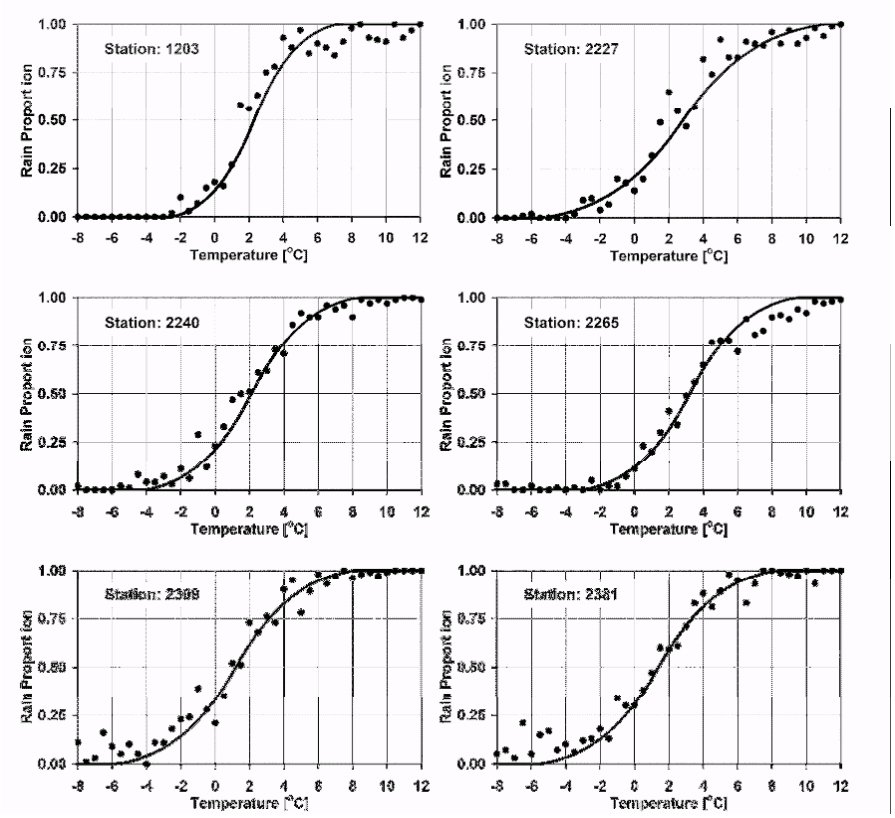

Figure 1. Snow and rain proportions versus daily mean temperature for six stations in south-west Alberta, with respective curvilinear fits

The procedure is to table all precipitation observations with the respective mean daily temperature, sort the table by temperature (using ½ degree temperature bins), and calculate the overall, or monthly, proportions of precipitation type for each temperature bin. The threshold temperature, where the proportion is 50%, and temperature range, which is the range in temperature between zero rain proportion and 100% rain proportion, can then be estimated (Figure 1). Empirical equations were developed, based on observations of 15 climate stations with long rain and snow records, to calculate, on a daily basis, the proportions of rain and snow:

for $T \leq T_T$ and $P_{Rain} \geq 0$:

$$P_{Rain} = 5 \times \left(\frac{T - T_T}{1.4 \times T_R}\right)^3 + 6.76 \times \left(\frac{T - T_T}{1.4 \times T_R}\right)^2 + 3.19 \times \left(\frac{T - T_T}{1.4 \times T_R}\right) + 0.5$$

for $T \geq T_T$ and $P_{Rain} \leq 1$:

$$P_{Rain} = 5 \times \left(\frac{T - T_T}{1.4 \times T_R}\right)^3 - 6.76 \times \left(\frac{T - T_T}{1.4 \times T_R}\right)^2 + 3.19 \times \left(\frac{T - T_T}{1.4 \times T_R}\right) + 0.5$$

where:

P_{Rain} = proportion of precipitation falling as rain, ranging from 0 to 1
T = mean daily air temperature near ground level, in °C
T_T = threshold temperature, where 50% of precipitation falls as rain, in °C, typically around 2°C
T_R = range of temperatures where both rainfall and snowfall can occur, in °C, typically around 13 °C

A sensitivity analysis, using a total of 963 years of daily precipitation observations, revealed that the sensitivity of the threshold temperature on mean annual snowfall estimations was quite similar for all climate stations. The change per degree T_T resulted in an average change in mean annual snowfall estimation of 8.7%, and a modest change in mean r^2 of 0.029. It was found that a change in T_R has little effect on the estimation of mean

annual snowfall, with average changes of 0.11% per degree increase in temperature range. However, T_R does affect the r^2 value. When one compares the coefficient of determination of estimates with a T_R of zero with estimates based on the best T_R, the average improvement is an increase in the r^2 value of 0.064.

A series of verification analyses was carried out, investigating the success of estimating snowfall from precipitation records and ground air temperature using four different methods under four different input data conditions. Mean results of the three objective functions used are summarized in Tables 1, 2 and 3. Consistently, the newly proposed method resulted in the best estimation of mean annual snowfall (Table 1), although the static threshold method is a very close contender. Also consistently, the proposed method produces the highest r^2 values (Table 2). Consequently, the proposed method also results in the highest mean annual snow weighted coefficients of determination (Table 3).

Table 1**.** Percent error of mean annual snowfall estimations for all methods tested

Estimation Method	Static Threshold	Leavesley *et al.*	Pipes and Quick	Proposed method
Mean annual values for all stations	8.1	9.6	8.2	**7.1**
Observed annual values for each station	0.9	3.7	8.2	**0.2**
Observed monthly values for each station	3.8	6.5	8.2	**3.5**
Sine curve based monthly values for each station	2.8	12.8	8.2	**2.7**

Table 2**.** Mean coefficients of determination between estimated and observed daily snowfall for all methods tested

Estimation Method	Static Threshold	Leavesley *et al.*	Pipes and Quick	Proposed method
Mean annual values for all stations	0.754	0.778	0.781	**0.802**
Observed annual values for each station	0.733	0.769	0.781	**0.789**
Observed monthly values for each station	0.786	0.807	0.781	**0.828**
Sine curve based monthly values for each station	0.773	0.758	0.781	**0.821**

Table 3**.** Mean annual snowfall weighted coefficient of determination for all methods tested

Estimation Method	Static Threshold	Leavesley *et al.*	Pipes and Quick	Proposed method
Mean annual values for all stations	0.700	0.712	0.724	**0.750**
Observed annual values for each station	0.727	0.742	0.724	**0.788**
Observed monthly values for each station	0.757	0.760	0.724	**0.799**
Sine curve based monthly values for each station	0.752	0.674	0.724	**0.800**

Generally, both the threshold temperature and the temperature range within which mixed precipitation occur, decrease with an increase in elevation. Regression functions could be established for the St. Mary's watershed to modulate the threshold temperature and the temperature range across the watershed in order to derive

estimates for the threshold temperature and temperature range for each HRU. Using eight selected climate stations, the regression equation derived to determine the mean annual critical temperature, which is then distributed seasonally using a sine function (Kienzle, 2008), is:

$$TC_{Annual} = 25{,}770 * Elev^{-1.301}$$

where TC_{Annual} is the mean annual critical threshold temperature in °C, and Elev is elevation in m.

THE REQUIREMENT FOR AND CALCULATION OF TWO DAILY TEMPERATURES

Air temperature controls both precipitation and evapotranspiration, two of the three principal variables determining the water balance at any location. In order to be able to simulate snowpack development or streamflow, both precipitation and evapotranspiration need to be estimated. Observed temperature records can typically not be directly used for hydrological simulations. This is due to the distribution of the climate stations, which are, as everywhere else in the world, situated for ease of access rather than to represent the full range of elevations and associated climatic conditions. This results in a bias towards representing lower elevations, particularly in regions with high relief.

The consequences are that the snow to rain proportions observed at the climate stations cannot be transferred to locations with distinctly different elevations. Therefore, the air temperature measured near the ground is generally used as the determining factor for the partition of precipitation into snow, mixed precipitation, or rain (e.g. Rachner and Matthäus, 1984; Braun, 1985; Vehviläinen, 1992; Rachner *et al.*,1997). When temperature values are required where no measurements are available, lapse rates are commonly used to adjust the minimum and maximum temperatures measured at the nearest climate stations to the location under consideration. The use of mean annual lapse rates must be avoided, as lapse rates typically fluctuate strongly during the course of a season. Mean monthly lapse rates can be estimated from surrounding climate stations, or, where available, calculated from monthly PRISM surfaces of minimum and maximum temperatures (Figure 2).

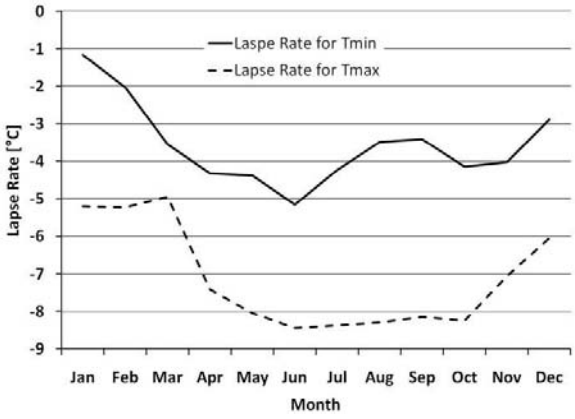

Figure 2. Monthly variation of lapse rates in the St. Mary watershed, Montana, estimated from PRISM monthly temperature surfaces

Following a new approach, it is suggested that the resulting lapse rate adjusted daily air temperatures from the base station are only used for the separation of precipitation into snow and rain. It is assumed that snowmelt and evapotranspiration, on the other hand, depend largely on the exposition of the local slopes, as well as land cover, as both have a strong influence on near-ground temperatures.

In order to enable different daily air temperatures as a function of exposition, i.e. north vs. south facing slopes or valleys that rarely receive direct incoming radiation, the lapse rate adjusted air temperatures need to be further adjusted according to exposition and land cover. Glassy and Running (1994) follow an approach that uses incoming radiation, which performs like an integrator of slope and aspect into one variable. A variation of their approach, used in MTCLIM (Thornton et al., 1997), is presented here, where the diurnal temperature range is used as a quantifier for temperature adjustments. Here, incoming radiation is calculated for every ½ hour in a GIS, based

on latitude, topography, hemispherical viewshed, atmospheric transmittivity, proportion of diffuse radiation, and elevation. Atmospheric transmittivity and diffuse radiation are changed on a monthly basis, using values from the nearest climate stations that record them. In this case, three climate stations were used that were within 150 km.

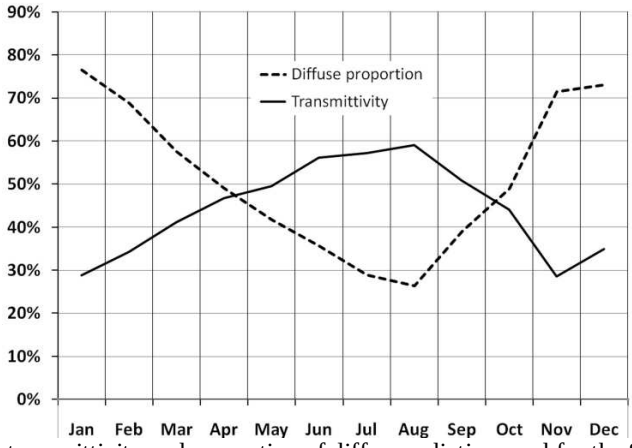

Figure 3. Atmospheric transmittivity and proportion of diffuse radiation used for the St. Mary watershed

Atmospheric transmittivity values are lowest between November and February, with values under 35%, reaching as low as 28%, and are highest between June and September, with values over 50%, getting as high as 59%. The proportion of diffuse radiation ranges from 77% to 26%, with highest values over 70% from November to March, and lowest values below 30% in July and August. Monthly incoming radiation was calculated in the GIS twice: once for the true, sloped topography, and once for the flat topography, assuming that DEM grid cells have all zero slope, thus still adjusting for atmospheric transmittivity and shading effects, but not for slope or aspect. All DEM derived values were then averaged over each HRU. The radiation ratio is calculated as follows:

$$RadRatio = (Rad_{Slope} - Rad_{Flat}) / Rad_{Flat}$$

This results in positive values, where Rad_{Slope} is greater than Rad_{Flat}, and negative values, where Rad_{Slope} is smaller than Rad_{Flat}. Other authors, such as Yang and Xiao (2008), have suggested an approach as to how carry out the temperature corrections. Yang and Xiao (2008) used the monthly mean temperature and multiplied it with the radiation ratio to derive the adjustment temperature. This approach cannot be used in cold climates, as the more the monthly mean temperatures approach zero degrees, the less the temperature correction would be. Here, daily minimum and maximum temperatures are then adjusted as follows:

$$T_{maxadj} = T_{max} + (T_{Range} / 2 * RadRatio)$$
$$T_{minadj} = T_{min} + (T_{Range} / 2 * RadRatio)$$

with:
T_{minadj} = radiation adjusted daily minimum air temperature
T_{maxadj} = radiation adjusted daily maximum air temperature
T_{Range} = daily temperature range ($T_{max} - T_{min}$)

The inclusion of the temperature range is based on the assumption that, under overcast conditions, T_{Range} is small and that the radiation influence is small, and that under clear sky conditions T_{Range} is large, and thus the radiation influence is large. It needs to be debated, whether the halving of the T_{Range} provides realistic results over a wide range of conditions. A first verification analysis based on observed temperatures, taken at various aspects and slopes in the vicinity of the study area, showed realistic temperatures on north and south facing slopes (Letts, University of Lethbridge, personal communication, 2008). Figure 3 presents the simple relationship between the daily temperature range and the radiation correction factor with the temperature adjustment.

In a second step, radiation adjusted daily minimum and maximum temperatures are further adjusted as a function of the leaf area index (LAI), as suggested by Glassy and Running (1994). As the LAI varies seasonally, the LAI is changed on a monthly basis. The source for LAI data was MODIS (2009). Figure 4 shows radiation input for July (4a), the radiation correction factor (4b), and unadjusted (4c) and adjusted (4d) mean annual maximum

temperatures. It must be noted that Figures 4a and 4b are based on a 100m DEM, while Figures 4c and 4d are based on larger, irregular shaped HRUs. The boxes in Figures 4c and 4d are included for easier comparison. The adjusted

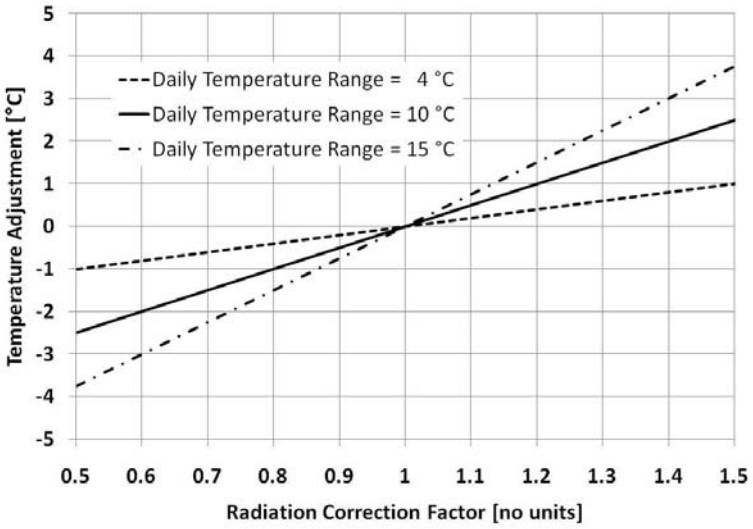

Figure 3. Dependence of the temperature adjustment on daily temperature range and the radiation correction factor

temperatures are higher on south-facing slopes (left box), lower on north-facing slopes (right box). The larger box shows that in the unadjusted scenario, temperatures follow the elevation contour lines, while the adjusted scenario results in a more complex temperature pattern, which is the result of radiation fluxes and land cover influences.

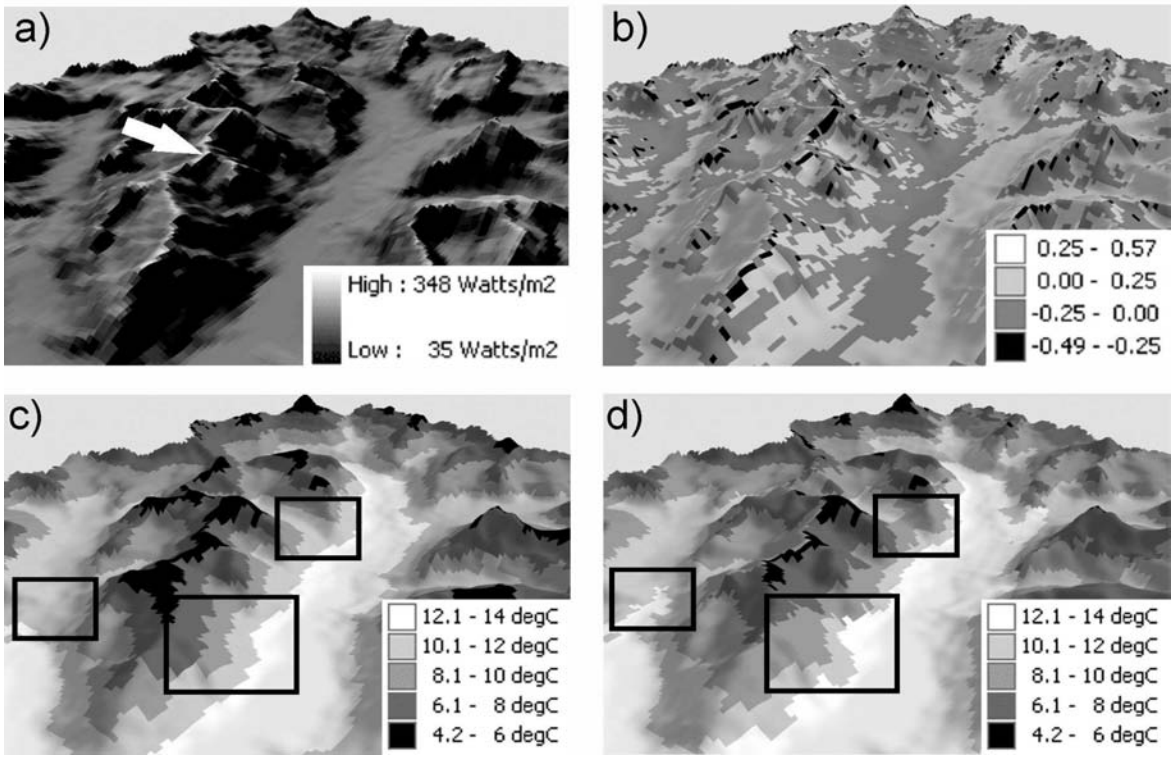

Figure 4. Radiation input for July (a), the radiation correction factor (b), and unadjusted (c) and adjusted (d) mean annual maximum temperatures (white arrow in (a) points North)

THE REQUIREMENT TO CORRECT SLOPED AREAS IN HYDROLOGICAL MODELING

It is interesting to observe that some fundamental area calculations required in hydrology appear to have been forgotten. The fact that sloped areas, when projected to a planimetric plane, have a smaller area than the true, sloped surface area was described by Strahler in 1956. He noted that the relationship between the so-called true surface area to that of the planimetric area can be described mathematically:

$$Area_{True} = Area_{Planimetric} / (COS(Slope))$$

where $Area_{True}$ and $Area_{Planimetric}$ are in any area units, and Slope is in degrees. This method is described in more detail by Rasmussen and Ffolliott (1981). When this equation is applied in a GIS, such as ArcGIS, the degrees need to be converted to radians by multiplying the slope in degrees by Pi and dividing by 180 (i.e. 3.1416/180).

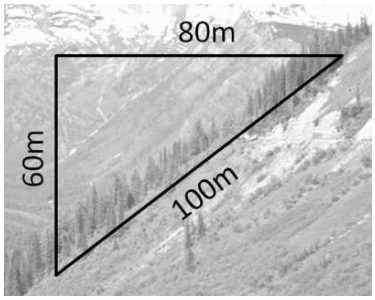

Figure 5. The sloped length is always longer than the horizontal length; the example with a slope area under-estimation factor of 25% is from Glacier National Park, Montana; here, the slope is about 37° or 75%.

Only few researchers have reported the correction of the planimetric area, as it is represented in digital elevation models and analyses with a GIS. For example, Guzzetti *et al*. (1997) computed the under-estimated areas for several watersheds in the north-central Po Plain in northern Italy and reported an underestimation of 5 – 9% for the steepest basins. Duart and Marquinex (2002), as well as Wichmann and Becht (2003), applied the same principle for geomorphological analyses of rockfalls in northern Spain, and the German Alps respectively, to determine the "actual surface area", using GIS analyses.

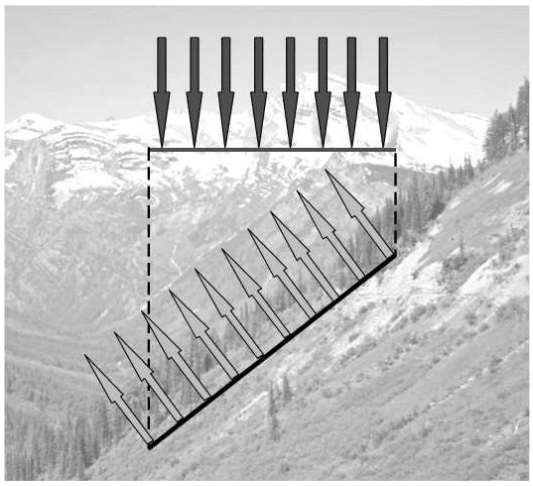

Figure 6. Hydrological inputs are distributed over a larger area on sloped surfaces; the output area is larger than the input area.

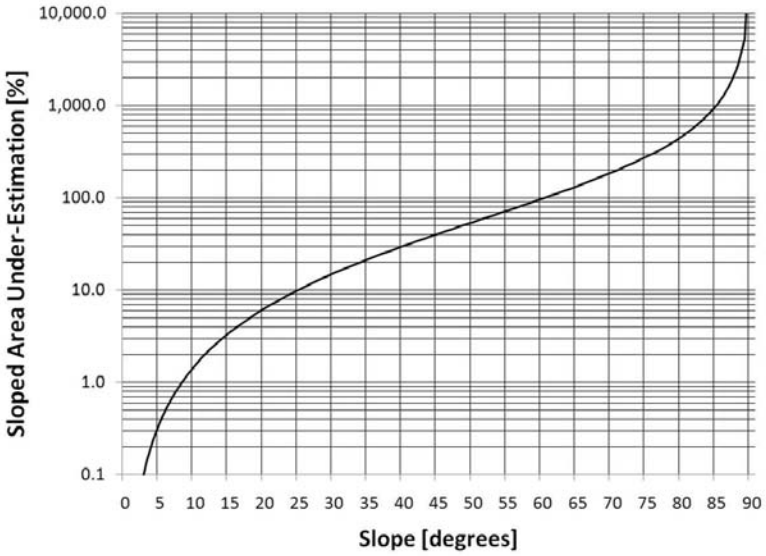

Figure 7. Graphical relationship between slope and the sloped area under-estimation factor

The omission of correcting the GIS derived areas for slope can have fundamental consequences in hydrological computations. Very few hydrological researchers have computed the impacts of a slope corrected "true area" in hydrological analyses. For example, Hopkinson *et al*. (2007) have analyzed glacial ablation rates using a GIS based surface area correction factor. Another glaciologist, Jiskoot (2009), is also correcting the planimetric areas provided by DEMs for slope under-estimation to calculate energy balances and ablation rates in glaciers.

The hydrological consequences can be significant, as the precipitation depth is distributed over a larger area, and all soil and vegetation related hydrological variables are also larger. Consequently, on a sloped surface, precipitation depth, infiltration depth, and groundwater recharge depth are reduced, while interception, soil water holding capacity, snowmelt, sublimation, evaporation and transpiration are increased. In other words, while the hydrological input remains the same, the hydrological outputs can be much larger on sloped terrain. Figure 7 shows the relationship between the slope and the sloped area under-estimation factor (SAUEF). It is evident that the SAUEF is very small when slopes are less than 10°. The hydrological effects become considerable with slopes over 25°, when the SAUEF is over 10%, which may be larger than many hydrological variables measured or estimated for that particular HRU. A 45° slope has a SAUEF of 40%, and slopes over 60° have a SAUEF of over 100%, and eventually approach infinity near vertical cliffs.

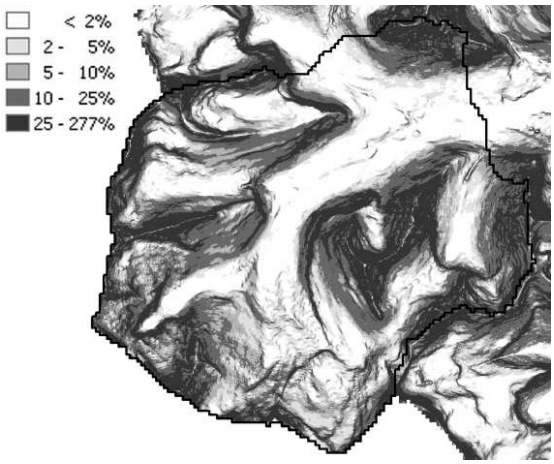

Figure 8. Sloped area under-estimation factor for a small watershed in Glacier National park, Montana (the watershed boundary is in black)

A small watershed in Glacier National Park in Montana was chosen to analyze the magnitude of the SAEUF. The watershed is located upstream of St. Mary Lake and is approximately 100 km2 in size. It is a typical Rocky Mountain watershed, encompassing steep valleys and sharp mountain peaks. A digital elevation model with a 10m grid cell size was used to calculate slope and the SAUEF. It is important to use high-resolution DEMs, as DEMs with a grid cell size larger than 30m would result in potentially significant under-estimation of the slope itself (Kienzle, 2004), and subsequently the SAUEF would also be under-estimated. Kienzle (2004) reported that the slope derived from a 30m DEM can be over 50% less than the slope derived from a 10m DEM, thus resulting in a potentially large under-estimation of the SAUEF. For example, if a slope derived from a 30m DEM was 30%, and the slope derived from a 10m DEM was 45%, the SAUEF would be 110% larger using a 10m DEM when compared to the 30m DEM. While the mean SAUEF of the test watershed does not change much with grid cell size, both the maximum and standard deviation do change considerably. This means that a relatively coarse DEM with a 100m grid cell size can be used with reasonably success to compute mean SAUEFs. However, steep areas, which have the largest slope area under-estimation factors, are potentially largely under-estimated.

Based on the 10 m resolution DEM, the test watershed has a mean SAUEF of 17.3%, and almost 50% of the watershed area has a SAUEF of 10% or more, and 23% of the watershed area has a SAUEF of 25% or higher, reaching as high as 1,050%.

The integrated effects on various hydrological processes are under investigation and will be reported on shortly.

CONCLUSIONS

For many years, GISs have been used to improve the spatial distribution of hydrological variables. Three advances in spatial modelling are presented here to improve the simulation of snowfall and snowmelt, and were incorporated in the ACRU agro-hydrological modelling system. The separation of precipitation into snow and rain depends on air temperature. Therefore, it is not only important to spatially represent air temperature realistically, but also to use the best possible way to separate snow and rain. A new method is described that appears to improve the modeling of snow from air temperature and total precipitation (Kienzle, 2008). As this method depends on adequate air temperature representation over the entire watershed on at least a daily basis, a new method is introduced that incorporates two daily temperatures to distinguish between temperatures that govern precipitation type and temperatures that govern hydrological processes on the ground, such as evapotranspiration and snowmelt. Lastly, the requirement for, calculation of, and incorporation of two areas for each HRU, are presented. This last method alone has the potential to greatly improve the hydrological representation and simulation of watersheds.

ACKNOWLEDGEMENTS

Some of the ACRU upgrades and pre- and post-processing routines were funded by the Alberta Ingenuity Centre for Water Research (AICWR Fund 42321) and by EPCOR/NSERC Fund 40286.

REFERENCES

ACRU 2007: The ACRU Model: Home Page. http://www.beeh.unp.ac.za/acru/. Last accessed 11/28/2007.

Braun, L.N. 1985. Simulation of snowmelt-runoff in lowland and lower alpine regions of Switzerland. Dissert. Zűrcher Geographische Schriften, Heft 21. (ETH) Zűrich.

Duarte, R.M., and J. Marquinez. 2002. The influence of environmental and lithologic factors on rockfall at a regional scale: an evaluation using GIS. Geomorphology, 43: 117-136.

Glassy, J., and S.W. Running. 1994. Validating diurnal climatology logic of the MT-CLIM logic across a climatic gradient of Oregon. Ecological Applications, 4: 248-257.

Guzzetti, F., M. Marchetti, and P. Reichenbach . 1997. Large alluvial fans in the north-central PO Plain (Northern Italy). Geomorphology 18: 119-136.

Hopkinson, C., L. Chasmer, S. Munro, and M. Demuth. 2007. Scale biases in glacial melt estimates using a GIS energy balance model and a lidar-derived DEM. In: CMOS, CGU, AMS Congress 2007: Air, Ocean, Earth and Ice on the Rock. May 28 - June 1, 2007, St. John's Congress Centre, Newfoundland and Labrador, Canada. I11-4C1 .4.

Jiskoot, H., C.M. Curran, D.L. Tessler, and L.R. Shenton. In press. Changes in Clemenceau Icefield and Chaba Group glaciers, Canadian Rocky Mountains, related to hypsometry, tributary detachment and slope-area-aspect relations. Annals of Glaciology 50 (53).

Kienzle, S.W. 2004. The effect of DEM raster resolution on first order, second order and compound terrain derivatives. Transactions in GIS, 8(1):83-111.

Kienzle, S.W. 1996. Using DTMs and GIS to define input variables for hydrological and geomorphological analysis. In: HydroGIS 96: Application of Geographical Information Systems in Hydrology and Water Resources Management (Proc. of the Vienna Conference, Austria, April 1996). IAHS Publications no. 235: 183-190.

Kienzle, S.W. 1993. Application of a GIS for simulating hydrological responses in developing regions. In: HydroGIS 93: Application of Geographical Information Systems in Hydrology and Water Resources Management (Proc. of the Vienna Conference, Austria, April 1993). IAHS Publications no. 211: 309-318.

Kienzle, S.W., S.W. Lorentz, and R.E.Schulze. 1997. Hydrology and Water Quality of the Mgeni catchment. Water Research Commission, Pretoria, Report TT87/97.

Kienzle, S.W., and R.E. Schulze. 1991. The simulation of the effect of afforestation on shallow ground water in deep sandy soils. Water SA 18(4): 265-272.

Kienzle. S.W., and J. Schmidt. 2008. Hydrological impacts of irrigated agriculture in the Manuherikia Catchment, Otago, New Zealand, Journal of Hydrology (NZ), 47(2):67-83.

MODIS (Moderate Resolution Imaging Spectroradiometer). 2009. Available at http://modis.gsfc.nasa.gov/data/, accessed Feb. 17, 2009.

New, M. 2002. Climate change and water resources in the southwestern Cape, South Africa. South African Journal of Science 98: 1-8.

Rasmussen WO and Ffolliott PF 1981: Surface area calculations applied to a resource map. Water Resources Bulletin, Vol. 17 (6): 1079-1082.

Rachner, M., and H. Matthäus. 1984. Snow hydrological research results in the German Democratic Republic and their applications for water resources management (in German: Schneehydrologische Untersuchungsergebnisse in der DDR und deren Anwendung fűr wasserwirtschaftliche Zwecke). DVWK-Mitteilungen 7: 235–255.

Rachner, M., H. Matthäus, and G. Schneider. 1997: Real-time forecasts of snowpack developments and snow ablation: First results of the project SNOWD (in German: Echtzeitvorhersage der Schneedeckenentwicklung und der Wasserabgabe aus der Schneedecke. Erste Ergebnisse aus dem Projekt SNOWD). Deutsche Gewässerkundliche Mitteilungen 41: 98–106.

Schulze, R.E. 1989. ACRU. Background Concepts and Theory. ACRU Report No. 36, Dept. Agric. Eng., Univ. of Natal, Pietermaritzburg, RSA.

Schulze, R.E. 1995. Hydrology and Agrohydrology: A Text to Accompany the ACRU 3.00 Agrohydrological Modelling System. Water Research Commission Report TT 69/95, Water Research Commission, Pretoria, Republic of South Africa.

Schulze, R.E., S. Lorentz, S.W. Kienzle, and L. Perks. 2004. Modelling the impacts of land-use and climate change on hydrological responses in the mixed underdeveloped / developed Mgeni catchment, South Africa. In: Kabat, P. *et al.* (Eds.): Vegetation, Water, Humans and the Climate A New Perspective on an Interactive System. BAHC-IGBP Publication, Springer.

Schulze, R.E., N.W. Schäfer, S.D.and Lynch. 1990. An assessment of regional runoff production in Qwa Qwa: a GIS application of the ACRU modelling system. South African Journal of Photogrammetry, Remote Sensing, and Cartography 15: 141–148.

Smithers, J., and R.E. Schulze. 1995. ACRU Agrohydrological Modelling System User Manual. WRC Report TT 70/95, Water Research Commission, Pretoria.

Smithers, J., R.E. Schulze, and S.W. Kienzle. 1997. Design flood estimation using a modelling approach: A case study using the ACRU model. In: Rosbjerg, D.; Boutayeb, N.; Gustard, A.; Kundzewicz, Z.W.; Rasmussen, P.F. (eds.) Sustainability of Water Resources under Increasing Uncertainty. IAHS Publication 240: 277-286

Smithers, J.C., R.E. Schulze, A. Pike, and G.P.W. Jewitt. 2001. A hydrological perspective in the February 2000 floods: a case study in the Sabie river catchment. Water SA 27 (3): 325-332. Gezina, South Africa.

Strahler, A.N. 1956. Quantitative slope analysis, Bulletin of the Geological Society of America, 67: 571-96.

Tarboton, K.C., and R.E. Schulze. 1993. Hydrological consequences of development scenarios for the Mgeni catchment. Proceedings of the Sixth South African National Hydrological Symposium, University of Natal, Pietermaritzburg, Department of Agricultural Engineering, 297–304.

Thornton, P.E., S.W. Running, and M.W. White. 1997. Generating surfaces of daily meteorological variables over large regions of complex terrain. Journal of Hydrology 190: 214–251

Vehviläinen, B. 1992. Snow cover models in operational watershed forecasting. Publications of the Water and Environment Research Institute, National Board of Waters and the Environment, Finland, Helsinki, 11: 112.

Wichmann, V., and M. Becht. 2003. Modeling of geomorphic processes in an alpine catchment. In: Conf. Proc. GeoComputation 2003 (Southampton, UK). http://www.geocomputation.org/2003/index.html

Yang, X., and C. Xiao. 2008. Terrain-based revision of an air temperature model in mountain areas. In: Zhou, Q., B. Lees, and G. Tang (Eds.): Advances in digital terrain analysis, Lecture Notes in Geoinformation and Cartography, Springer, 462 pp.